This article was published as

Phil. Trans. R. Soc. A 378: 20190255 (2020)

DOI: http://dx.doi.org/10.1098/rsta.2019.0255

PHILOSOPHICAL TRANSACTIONS A

Phil. Trans. R. Soc. A.
doi:10.1098/not yet assigned

Rheology of magnetic colloids containing clusters of particle platelets and polymer nanofibers

Mariem Mekni Abrougui[1], Ezzeddine Srasra[1], Modesto T. Lopez-Lopez[2,#] and Juan D. G. Duran[2,*]

[1]Centre National des Recherches en Sciences des Materiaux, Technopole Borej Cedria, BP 73, 8027 Soliman, Tunisia; and Faculté des Sciences de Tunis, Université de Tunis El Manar, Tunisie B.P. 94-Rommana, 1068, Tunisia
[2] Department of Applied Physics, Faculty of Sciences, University of Granada, 18071, Granada, Spain.
#ORCID ID 0000-0002-9068-7795; *ORCID ID 0000-0002-5586-1276

Keywords: Hydrogel, ferrogel, magnetorheology, bentonite, magnetite, alginate.

Summary

Magnetic hydrogels (ferrogels) are soft materials with a wide range of applications, especially in biomedicine because: (i) They can be provided with the required biocompatibility; (ii) their heterogeneous structure allows their use as scaffolds for tissue engineering; (iii) their mechanical properties can be modified by changing different design parameters or by the action of magnetic fields. These characteristics confer them unique properties for acting as patterns that mimic the architecture of biological systems. In addition, (iv) given their high porosity and aqueous content, ferrogels can be loaded with drugs and guided toward specific targets for local (non-systemic) pharmaceutical treatments. The ferrogels prepared in this work contain magnetic particles obtained by precipitation of magnetite nanoparticles onto the porous surface of bentonite platelets. Then, the particles were functionalized by adsorption of alginate molecules and dispersed in an aqueous solution of sodium alginate. Finally, the gelation was promoted by crosslinking the alginate molecules with Ca^{2+} ions. The viscoelastic properties of the ferrogels were measured in the absence/presence of external magnetic fields, showing that these ferrogels exhibited a strong enough magnetorheological effect. This behaviour is explained considering the field-induced strengthening of the heterogeneous (particle-polymer) network generated inside the ferrogel.

1. Introduction

The development of biocompatible hydrogels has received considerable attention in last few decades due to a series of biomedical applications, among which it is worth mentioning their use as scaffolds in tissue engineering [1-3], for example bone or cartilage regeneration [4, 5], or alternatively as carriers for local drug delivery in cancer therapy [6].

Hydrogels can be defined as polymeric networks, capable of absorbing and retaining high amounts of aqueous solutions, without being dissolved in the liquid media. Usually, the polymer chains form three-dimensional structures generated by (chemical or physical) crosslinking among the polymer molecules. However, most hydrogels suffer from a lack of mechanical strength, which usually limits their applications in a

*Author for correspondence (jdgarcia@ugr.es).
†Present address: Department of Applied Physics,
Faculty of Sciences, University of Granada, 18071, Granada, Spain

variety of fields. Many efforts have been devoted to improving the stiffness of hydrogels. Among them, the combination of organic-inorganic compounds through blending of polymers with nanoparticles has received special attention because of its excellent mechanical resilience when compared with conventional hydrogels [7, 8]. In this context, the use of magnetic particles seems a promising approach because of their field-responsive properties [9, 10, 11]. In addition, the use of composite magnetic particles of low average density has been proved as a good way to avoid the heterogeneous distribution of the particles inside the ferrogels [12]. Furthermore, if the composite particles have low density and elongated shape (e. g. sepiolite-magnetite), the magnetic control of the mechanical properties of the resulting ferrogels can be considerably improved [13].

On the other hand, facing biomedical applications, natural polymers are usually preferred instead of synthetic ones because the satisfy the required biocompatibility of the resulting gels [10]. Among natural polymers, polysaccharides, peptides, and proteins have a demonstrated capability for generating these kind of soft-wet biomaterials [11-19]. In particular, alginate is a natural polysaccharide of particular interest because is soluble in water, relatively inexpensive, non-toxic, and biocompatible. The molecule of sodium alginate bears carboxylate groups and has the ability to form hydrogels by electrostatic interaction with divalent cations (especially Ca^{2+}) at room temperature. This kind of physical crosslinking is the key characteristic for the formation of the alginate hydrogels employed in the present work [20, 21].

The aim of the present work is to prepare, and study the physical properties, of ferrogels consisting of magnetic particles embedded into a matrix of alginate hydrogel. The magnetic particles were synthetic composites of low density containing a core of clay covered by magnetite nanoparticles. The clay chosen was bentonite because the particles of this mineral have a plate-like shape and, according to our previous experience [13], the magnetorheological (MR) response of ferrogels based on elongated particles can be significantly stronger than that of ferrogels based on spherical particles. In this paper, we first describe the synthesis of the clay-magnetite composites. Then, we analyse their more relevant physico-chemical characteristics (including magnetization curves) by different techniques. After that, we describe and discuss the rheological behaviour of both the bentonite-magnetite ("BMag" in what follows) aqueous suspensions and the BMag-alginate ferrogels, in the absence/presence of magnetic fields.

2. Materials and methods

(a) Materials

The raw bentonite material used in this study was collected from Zaghouan (Northeast of Tunisia). It was subjected to a purification process using the so-called hydrocyclone separation method, previously described in detail in refs. [22, 23]. This process allowed removing impurities present in the raw material (mainly calcite and quartz), and also the change of the original calcium exchange ions present in the clay mineral by sodium ones. The main characteristics of the purified bentonite employed in the present work were [22]: i) Bulk chemical composition, obtained by X-ray fluorescence, in weight percent: 49.28% SiO_2, 20.82% Al_2O_3, 6.98% Fe_2O_3, 3.74% CaO, 2.80% MgO, 1.94% Na_2O, 2.02% K_2O, 0.11% P_2O_5, 1.08% TiO_2, 0.02% MnO; ii) cation exchange capacity 64 meq/100g; iii) specific surface area 70 m^2/g; iv) the thickness (a) and length (L) of the bentonite platelets were (mean ± standard deviation) a = 0.33 ± 0.06 μm and L = 2.3 ± 0.4 μm, and the corresponding aspect ratio (a/L) = 0.14 ± 0.05.

The chemicals employed (supplied by Sigma-Aldrich, USA) in the synthesis of the composite bentonite-magnetite particles were: $FeCl_3 \cdot 6H_2O$ (98%), NH_4OH aqueous solution (25% NH_3), and $FeCl_2 \cdot 4H_2O$ (98%). For the preparation of the alginate hydrogels the reagents used, without further purification, were: sodium alginate (Across Organics, USA, Sigma Aldrich CAS number 9005-38-3), $CaCl_2$ (anhydrous, minimum 96.0%, Sigma Aldrich, USA), D-(+)-Gluconic acid δ-lactone (GLD) (> 99.0%, Sigma Aldrich, USA, CAS number 90-80-2), and

$CaCO_3$ (Sigma Aldrich). All the solutions and suspensions were prepared using Milli-Q quality deionized water (Milli-Q Academic, Millipore, France).

(b) Synthesis of the bentonite-magnetite particles and magnetite nanoparticles

The synthesis of the BMag composites was carried out, adapting a previous one reported in ref. [24] for attapulgite-magnetite composites, as described by the following steps:

i) Preparation of bentonite suspension in Fe^{3+} aqueous solution: 4.410 g of $FeCl_3 \cdot 6H_2O$ was dissolved in 200 mL of deionized water. Then, 1.5 g of bentonite was dispersed in the Fe^{3+} solution using an ultrasonic bath for 30 minutes until a stable suspension was obtained. After that, the suspension was deoxygenated by bubbling nitrogen for 15 min. The flask was closed and the suspension was magnetically stirred overnight.

ii) In the bentonite-Fe^{3+} suspension obtained in the previous step we added 1.614 g of $FeCl_2 \cdot 4H_2O$. This new suspension, containing Fe^{2+} ions in solution, was heated up to 90 °C. After that, 6 mL of NH_4OH solution was added rapidly under stirring. Immediately, a black precipitate appeared as a result of the formation of magnetite particles. Then, the suspension was kept under mechanical stirring in nitrogen atmosphere at 90 °C for 1 h. The resulting suspension was cooled down to room temperature.

iii) Finally, the BMag particles were washed. For this aim, the particles were settled using a powerful magnet. Then, the supernatant solution was discarded, and the particles redispersed in fresh water. This procedure was repeated until the conductivity of the supernatant was less than 20 µS/cm.

The synthesis of the magnetite nanoparticles was identical to that of the BMag particles, except for the following differences: in step i) the Fe^{3+} solution did not contain bentonite particles; in step iii) the repeated cycles of decantation/redispersion were carried out until the supernatant was at pH ≈ 7.

The samples notation with a brief description is included in Table 1.

(c) Preparation of the magnetic hydrogels

Previously to the preparation of the ferrogels, the BMag particles were functionalized by adsorption of alginate molecules. To this end, two different suspensions were prepared. In the first one, 1.0 g of BMag particles was dispersed into 50 mL of a solution containing 0.25 g (0.5% w/v) of sodium alginate. In the second one, 1.0 g of BMag particles was dispersed into 50 mL of a solution containing 1 g (2% w/v) of sodium alginate. After allowing 12 h for alginate adsorption on the particle surface, the particle were recuperated and washed following the procedure described in section 2(b), point (iii). (See sample notation in Table 1).

The BMag particles, functionalized by alginate adsorption (samples BMagF1 and BMagF2), were employed for the preparation of ferrogels. For this purpose, we followed the next steps:

i) The magnetic particles were dispersed in four different solutions of sodium alginate. In all these pregel suspensions the particle concentration was 10% w/v and the alginate concentrations were 0.25, 0.5, 1, and 2% w/v. These suspensions were shacked by hand until the suspensions were homogenous.

ii) After that, 22.5 mg of $CaCO_3$ and 26.7 mg of gluconic acid (GLD) were added to each suspension and the resulting mixture was shaken by hand. The role played by GDL was the slow acidification of the aqueous solution, by hydrolysis of this weak organic acid, allowing the gradual liberation of calcium ions from the $CaCO_3$. This controlled reaction favoured the homogeneous crosslinking of the alginate molecules, avoiding the formation of thick lumps into the ferrogels.

iii) Finally, 4 hours after the start of the previous step, the gelation process was completed by addition of a solution of $CaCl_2$ (5 mL, 45 mM concentration). The ferrogel was left at rest overnight at room temperature. The addition of this $CaCl_2$ solution provoked the swelling and the saturation of the crosslinking (by Ca^{2+} diffusion). Thus, ferrogels with enough tautness for handling were obtained.

(d) Experimental methods

The X-ray diffraction patterns (XRD) of bentonite (Bent) and bentonite covered by magnetite particles (BMag) were obtained in a Philips X'Pert Pro diffractometer (PANalytical, Netherlands) working on Kα monochromatic radiation of copper. In addition, the morphology of Bent and BMag particles was obtained by high resolution scanning electron microscopy (FESEM; Zeiss SUPRA40VP, USA).

Zeta potential measurements were carried out in a Malvern Zeta-Sizer Nano SZ (UK) at 25 °C. For these measurements, different suspensions containing 1% w/v particle concentration of Fe3O4, Bent, BMag, BMagF1, and BMagF2 (see Table 1) in aqueous media (1mM NaCl ionic strength; pH interval from 3 to 10), were prepared. These suspensions were left at rest for 24 h. To avoid the effect of the particle sedimentation the samples were redispersed in an ultrasound bath, and the pH readjusted, immediately before the measurements. The values reported correspond to the average ± standard deviation of at least nine measurements of different aliquots.

The magnetization of the dry powder of BMag particles was measured at room temperature in a VSM 4500 magnetometer (EG&G Princeton Applied Research, USA), by applying the following magnetic field intensity (H) sequence: 0 – 374 kA/m (first magnetization), followed by the cycle (magnetization loop) 374 – 0 – (-374) – 0 – 374 kA/m.

The rheological characterization of the suspensions and ferrogels was carried out in the presence and absence of applied magnetic field in a magnetorheometer (Physica Anton-Paar MCR 300, Germany) with a plate-plate geometry (rotor plate diameter 20 mm) at constant temperature of 25.0 ± 0.1 °C. The plates had a rough surface to avoid wall slipping. The magnetic field applied (intensity H = 156 kA/m or 282 kA/m) was perpendicular to the rheometer plates. The samples were placed in the bottom plate and a normal force of 0.1 N was kept on the disk-like samples to ensure a good contact among plates and samples; the gap between the plates was slightly different for different samples, in order to maintain this value of the normal force. A water vapour saturated atmosphere was maintained around the samples to minimize their drying. Furthermore, in order to ensure the same initial conditions, a fresh sample was employed in each measure and, in the case of the suspensions of BMag particles for minimizing the possible effect of the particle sedimentation, the samples were strongly redispersed before the measurements.

The viscoelastic moduli of the suspensions and hydrogels were obtained by application of an oscillatory (sinusoidal) shear stress to the samples and the subsequent measurement of the corresponding shear strain. In all these experiments the frequency was maintained at 1 Hz, and the shear stress amplitude was progressively increased until the non-linear viscoelastic region was reached. The time elapsed in each stress step was 5 s. From the values of the stress and strain amplitudes and the phase difference between shear and strain, the elastic or storage (G') and viscous or loss (G") moduli were obtained. These oscillatory measurements were performed under constant magnetic field applied (H = 0; or H = 156 kA/m; or H = 282 kA/m) during the total duration of the experiment. These field values do not correspond exactly to the internal field in the sample in the rheometer gap, but taking into account the relatively small particle volume fraction in the suspensions and ferrogels (4.05% v/v; see section 2b below), and consequently the small demagnetizing fields, both the internal and the external fields are very close.

3. Results and discussion

(a) Physicochemical characterization

The X-ray diffraction patterns of the particles in samples Bent, BMag, and Fe3O4 (Table 1) are represented in figure 1. For the Fe3O4 sample, the peaks at diffraction angles 2θ = 18.27°, 30.09°, 35.49°, 43.05°, 53.48°, 56.94°, and 62.72° correspond to the planes (111), (220), (311), (400), (442), (511), and (440) in the crystal lattice of pure magnetite. In the pattern of BMag sample remained the same peaks of pure magnetite and also appear at 2θ = 26.64° and 19.85° those of the bentonite core. Nevertheless, these peaks become wider and their intensity was reduced as compared with those in pure bentonite likely due to the (at least partial) coating by magnetite nanoparticles present in the BMag composites. Note that, as this technique does not allow distinguishing between magnetite and maghemite, the presence of maghemite in the BMag particles cannot be excluded.

The morphology of the composite particles can be seen in the SEM pictures of figure 2. The bentonite particles (figure 2a) appeared as twisted and stacked platelets with a great polydispersity in size. Figure 2b shows the BMag particles and, as observed, the primitive clay clusters exhibited a partial coverage by small (around 100-200 nm) bright spots. These tiny spots correspond to magnetite nanoparticles grown onto the clay surfaces, probably because the clay mesopores (remember that bentonite specific surface area was 70 m^2/g) acted as seeds that promoted the precipitation of magnetite during the synthesis process.

The zeta potential of the different particles (Fe3O4, Bent, BMag composites, and the functionalized BMagF1 and BMagF2), as a function of the pH of the aqueous medium, is plotted in figure 3. The zeta potential of the magnetite particles presented an isoelectric point at pH(iep) ≈ 6.5, which is in good agreement with those values previously reported in literature [25, 26] for magnetite nanoparticles obtained by coprecipitation. The zeta potential curve of bentonite particles follows the typical trend of smectite clays (bentonite or montmorillonite; sepiolite) and silica particles [13, 25-29], that is, the particles bear a negative surface charge (and negative zeta potential) in the entire pH range under study. In the case of the non-functionalized composite particles (sample BMag), the tendency observed is coherent with a surface electrochemistry that combines those of Bent and Fe3O4 samples. Note that the surface reactions that determine the zeta potential of these materials (magnetite, bentonite, clay-magnetite) have been summarized in our previous work [13]. Finally, the adsorption of the dissociated alginate molecules provoked a clear increase (in absolute value) of the zeta potential of the BMag substrate, more pronounced as the concentration of alginate in solution was increased, as shown in figure 3 in the curves for BMagF1 and BMagF2 suspensions. This effect is a consequence of the surface reactions, via formation of coordination compounds, among the carboxylate groups of the alginate ligands and the Fe(II), Fe (III), and Si(IV) cations in the particles surface. Really, these metal (M = Fe or Si) ions are present in the solid-solution interface as $M\text{-}O^-$ (basic pH), M-O-H (neutral pH), or $M\text{-}O\text{-}H_2^+$ (acid pH) and the alginate adsorption is even more favoured at acid pH by electrostatic attraction between the alginate molecules and the $M\text{-}O\text{-}H_2^+$ group. The formation of these surface alginate complexes on magnetite or bentonite particles have been extensively studied [30, 31], and similarly for other polyelectrolytes that also bear carboxylate groups (e.g. humic acids) on clay or hematite particles [30, 31].

The negative zeta potential of the functionalized particles has an additional advantage on the colloidal stability of the suspensions. As demonstrated in a previous work [25], the bentonite-magnetite platelets in aqueous suspensions suffer of a high degree of aggregation because the van der Waals attraction between the particles faces overcomes the electrostatic repulsion between them. In consequence, the particles form stacked clusters and settle by gravitational forces. However, if the particles are functionalized by alginate adsorption, the electro-steric repulsion avoids in a high extent their aggregation and the subsequent fast sedimentation.

Figure 4 showed the sedimentation of the bare and functionalized particles along one week, demonstrating that the settling of the bare (BMag) particles was considerably slowed by alginate adsorption (BMagF1, BMagF2 samples). As mentioned in section 2(d), to minimize the effect of the sedimentation, all the samples were strongly redispersed immediately before carrying the zeta potential and rheological measurements, which in any case take only a few minutes.

Figure 5 shows the magnetic response of the BMag particles (dry powder) when a magnetic field cycle is applied (figure 5a). As observed, the composite BMag particles developed strong enough magnetization. The saturation magnetization can be obtained by fitting the data in the first magnetization curve (figure 5b) to the the Frölich-Kennely equation [32]:

$$M = \frac{cM_S H}{M_S + cH} \qquad [1],$$

where χ is the magnetic susceptibility and M_S the saturation magnetization. Their estimated values are χ = 3.90 ± 0.05 and M_S = 110.0 ± 0.3 kA/m; coefficient of determination r^2 = 0.995. Considering the saturation magnetization of pure magnetite ($M_{S,m}$ = 446 kA/m [33]), and the mixing law [34]:

$$M_S = f M_{S,m} \qquad [2],$$

the estimated volume fraction (ϕ) of magnetic material in the BMag composite particles was ϕ = 24.7%. Taking for the density of bentonite and magnetite 2.1 g/cm^3 and 5.5 g/cm^3, respectively, the average density of the BMag particles was 2.5 g/cm^3. In addition, the data in figure 5 demonstrated that the powder behaved as a magnetically soft material because the magnetic hysteresis was practically negligible given that the remnant magnetization and the coercive field (M_R = 0.45 kA/m and H_C = -0.08 kA/m, respectively) are within the typical measurement error of the VSM magnetometer.

(b) Rheological characterization

The viscoelastic moduli for both the suspension of non-functionalized particles (BMag) and the different ferrogels prepared were obtained by applying a sinusoidal shear stress (oscillatory regime). All the samples studied contained a particle concentration of 10% w/v, equivalent to a particle volume fraction ϕ = 4.05% v/v. During the experiments a stationary and homogeneous external field was applied to the samples with magnetic intensities H = 0, or H = 156 kA/m, or H = 282 kA/m. Figure 6 shows the results corresponding to the suspension of BMag particles. In this figure we can clearly observe, whatever the field applied, two different regions: an initial psedoplateau, in which G′ is practically independent of the strain amplitude (γ_0) that corresponds to the linear viscoelastic region (LVR), followed by a second region (non-LVR) in which G′ suffers an abrupt decrease. In the first region, G′ is larger than G″ as corresponds to a typical viscoelastic solid. In the second region (non-LVR), as γ_0 increases, there is a progressive transition from a viscoelastic solid to a liquid one (G″ > G′). The critical point for this transition can be clearly identified, in the curves for H ≠ 0, at the critical strain in which G″ reaches its maximum value at $\gamma_0 \approx 0.6$ (or 60%). This point corresponds to the breaking of the internal microstructure of the suspensions, because at this point the mechanical forces corresponding to the shear applied overcome the magnetic attraction among the particles and rapidly the material loses its elastic response (G′ decreases), which favours the subsequent viscous flow of the suspension (increment in G″).

The magnetic field-induced enhancement of the G′ values within the LVR (the so-called magnetorheological effect, MRE) can be quantified by the equation:

$$\mathrm{MRE}(\%) = \frac{G'(H \neq 0) - G'(H = 0)}{G'(H = 0)} \cdot 100 \qquad [3].$$

Table 2 includes the values of MRE (%) for the two values of the field applied to this suspension: 76100% (at H = 156 kA/m) and 197200% (at H = 282 kA/m), which are enormous in comparison with those usually reached

in ferrogels as we will see below. Nevertheless, the quantification of the MR effect by equation [3] does not seem appropriate for nearly liquid-like suspension that in the absence of field has a very low elastic modulus (G' ~ 10 Pa). A more convenient quantification of the MR effect can be done considering the plastic viscosity (η) of the suspensions in the absence/presence of field applied, by means of:

$$\text{MRE-}h(\%) = \frac{h(H \neq 0) - h(H = 0)}{h(H = 0)} \times 100 \qquad [4].$$

The plastic viscosities were obtained form the slope of the shear stress vs. shear rate rheograms (not shown for brevity) by linear fitting in the shear rate interval from 1 to 50 s^{-1}. The values of the plastic viscosities and the corresponding MR effect calculated by equation [4] are included in Table 1. Now, the MRE-η value reached for the maximum field is 87%, which appears a more reasonable estimation.

For the ferrogels prepared in this work, first we will analyse the viscoelastic behaviour in absence of magnetic field. In figure 7 the values of the viscoelastic moduli are plotted as a function of γ_0. Figure 7a includes the results for the samples BMagF1+X%Alg that contains 10% w/v of functionalized particles (BMagF1) embedded in hydrogels prepared with increasing concentrations of alginate (from 0.25 to 2% w/v alginate; see Table 1) in the pregel solution. From this figure 7a, it seems evident the pronounced effect of the alginate concentration on the mechanical properties of the resulting hydrogels. The increase of the alginate concentration from 0.25 to 2% w/v provoked an increase in the G' values corresponding to the LVR (see solid symbols in figure 7a) of around two orders of magnitude. For the BMag particles functionalized with a larger amount of adsorbed alginate, the viscoelastic moduli of all the ferrogels (samples BMagF2+X%Alg, figure 7b) are even higher: see the exact values of G' for these samples in Table 2.

Therefore, up to this point we have two different mechanisms to control the mechanical moduli of the ferrogels: the amount of alginate adsorbed on the particles and the concentration of alginate in the pregel solution. This behaviour can be explained considering, as demonstrated in a previous work [13], the crosslinking (by calcium ions) among the alginate molecules adsorbed onto the particles and those present in the pregel solution, which favours the networking among the particles and the polymer fibres. As a consequence, the resulting ferrogels consist of a network of alginate fibres in which the magnetic particles are not only randomly dispersed but act as knots that reinforce the elasticity of the material.

A third mechanism, as for magnetorheological suspensions, is the action of an external magnetic field of enough intensity. In this work the fields applied were H = 156 kA/m and H = 282 kA/m, both of them below (but not too far) the field required to reach the magnetic saturation of the particles; see in figure 5 that the field intensity for the maximum magnetization is above H = 400 kA/m.

In figure 8 we plotted the viscoelastic moduli of the samples BMagF2+0.25%Alg (figure 8a) and BMagF2+2%Alg (figure 8b) for the different fields applied. As observed (see also Table 2), for the weakest ferrogel (0.25% alginate) there is a significant effect of the field-induced attraction among the particles that gave MRE values (equation 3) of 84% (H = 156 kA/m) and 167% (H = 282 kA/m). On the contrary, the values of MRE (%) are considerably smaller for the most concentrated hydrogel (BMagF2+2%Alg, Table 2) in which MRE (%) are 4% and 12% for H = 156 kA/m and H = 282 kA/m, respectively. In this case, the curves obtained for different fields applied tend to collapse (see figure 8b).

Nevertheless, the data in Table 2 shows that the maximum magnetorheological effect was reached for an intermediate value of the alginate concentration (sample BMagF2+0.5%Alg) with MRE values of 181% (H = 156 kA/m) and 520% (H = 156 kA/m). For this sample, the polymer network seems to be still weak enough to allow a strong field-induced reinforcement of the ferrogel.

Summarizing, the application of an external magnetic field allows a strong MR effect only if the hydrogel network is not too dense. However, if the particles are entangled in a highly concentrated hydrogel their field-induced approaching is practically hindered and the deformation of the ferrogel mainly depends on the resilience of the polymer-particles network, being negligible the role played by the magnetic interactions.

Finally, it is convenient to analyse the influence of the shape of the magnetic particles on the magnetic control of the rheological properties of the ferrogels. Thus, we have to separate the shape effect from other quantities as the particle concentration, the intensity of the field, and the magnetization of the particles. For this purpose, we can consider that, according to the magnetorheological model proposed by Ginder et al. [35] (see also ref. [36]), the shear modulus depends linearly on the field applied (H), the particle volume fraction (Φ), and the particle magnetization saturation (M_S). Although this model is based on a number of restrictive assumptions (particle volume fraction Φ < 20% – 30%; linear field-induced chaining of spherical particles; intermediate field, well below the field for saturation magnetization; very low strain), it can be useful to define a normalized MR effect parameter as [13]:

$$\overline{MRE(\%)} = (MRE)(\%)\frac{M_{S,0}}{M_S}\frac{H_0}{H}\frac{\Phi_0}{\Phi} \qquad [5].$$

Here the quantities H, M_S and Φ corresponds to those of the ferrogels studied in refs. [13, 16, 37] and the quantities with subscript "0" correspond to the ferrogel BMagF2+0.5%Alg prepared in this work. All these data are included in Table 3.

The data in Tables 2 and 3 demonstrate that:

i) The ferrogels prepared with plate-like magnetic particles (bentonite-magnetite) can provide a very high MR effect when the alginate concentration was not too high. The maximum field effect (MRE = 520%) is achieved at 0.5% w/v alginate concentration in the pregel solution.

ii) The alginate concentration in the pregel solution determines in a great extent (and allows a wide control of) the MRE values achieved in the ferrogels containing functionalized magnetic platelets.

iii) If we compare ferrogels containing particles with different shapes (bentonite-magnetite platelets, sepiolite-magnetite fibres, silica-iron spheres) and equal alginate concentration (1% w/v) in the pregel solution, the maximum field effect corresponds to those with fibre-like composite particles. The normalized MRE values are: 21% (platelets), 180% (fibres), and 43% (spheres).

4. Conclusions

Hydrogels containing biocompatible polymer fibres and magnetic micro- or nanoparticles are very promising soft-wet materials for biomedical applications because their internal microstructure can work as patterns (or extracellular matrix or scaffolds, in the terminology used in tissue engineering) for generating soft biological tissues. The configuration of such internal structure depends on a number of variables that allows controlling their macroscopic properties as the mechanical moduli and the hydration degree. These variables are mainly: i) the length and crosslinking degree of the polymer fibres; ii) the crosslinking degree among the polymer fibres and the molecules adsorbed onto the solid particles; iii) the kind of bond (covalent, electrostatic) between the crosslinker and the polymer molecules; iv) the volume fraction of solid particles embedded into the hydrogel; v) the magnetic properties of the particles; vi) the intensity of the applied magnetic field.

In this work the crosslinker agent employed was calcium ions and the interaction among the alginate molecules was electrostatic. This physical crosslinking favoured the formation of soft and easy to handle hydrogels, which elasticity can be controlled in a wide range by varying the alginate concentration in the pregel solution. Even more, when the particles were functionalized by adsorption of alginate molecules onto the particle surface, the solid particles occupied the knots of the internal network, so avoiding the settling of the particles inside the gel. Simultaneously, this particle-polymer networking reinforced the mechanical response of the gel under the action of mechanical stresses.

The magnetic particles embedded in the hydrogels prepared in this work were composites of bentonite platelets on which magnetite nanoparticles were synthetized by a coprecipitation reaction. These composite particles were functionalized by adsorption of alginate molecules and the resulting particles had low density and, consequently, negligible settling rate inside the pregel solution. This fact allowed obtaining homogeneous ferrogels with a high enough magnetorheological effect. Nevertheless, the intensity of that MR effect strongly depended on the concentration of sodium alginate employed for the preparation of the pregel solution, being the optimal concentration 0.5% w/v.

The comparison of the ferrogels based on magnetic particles with different shapes and the same alginate concentration –normalizing other quantities as particle concentration, field applied, and magnetization– demonstrated that the more intense MR effect is achieved with fibre-like particles. The MR effect attained for spherical and plate-like particles were of same order of magnitude possibly because some stacked clay clusters remained in the ferrogels, in spite of the electro-steric stabilization imparted by the adsorbed alginate molecules. However, the use of magnetic composites based on clay minerals has the advantage, in comparison with spherical particles of pure magnetite or iron, of avoiding the settling of the particles inside the pregel suspension, so providing ferrogels with high homogeneity. And this property (homogeneity) is an essential condition for the generation of good artificial tissues that mimic the native ones by cell culture inside biocompatible hydrogels.

Acknowledgments. The authors are also grateful to Dr. Pavel Kuzhir (Institut de Physique de Nice, Université Côte d'Azur, CNRS; Nice, France) for his help in measuring the magnetic properties of the powder. This study was supported by project FIS2017-85954-R (Ministerio de Economía, Industria y Competitividad, MINECO, and Agencia Estatal de Investigación, AEI, Spain, cofunded by Fondo Europeo de Desarrollo Regional, FEDER, European Union).

5. References

1. Van Vlierberghe S, Dubruel P, Schacht E. 2011. Biopolymer-based hydrogels as scaffolds for tissue engineering applications: a review. *Biomacromolecules* **12**, 1387–1408. (doi:10.1021/bm200083n)
2. Gahawar AK, Peppas NA, Khademhosseini A. 2014. Nanocomposite hydrogels for biomedical applications. *Biotechnol. Bioeng.* **111**, 441–453. (doi:10.1002/bit.25160)
3. Ismail YA, Martínez JG, Al Harrasi AS, Kim SJ, Otero TF. 2011. Sensing characteristics of a conducting polymer/hydrogel hybrid microfiber artificial muscle. *Sens. Actuators B* **160**, 1180-1190. (doi:10.1016/j.snb.2011.09.044)
4. Rezwan K, Chen QZ, Blaker JJ, Boccaccini AR. 2006. Biodegradable and bioactive porous polymer/inorganic composite scaffolds for bone tissue engineering. *Biomaterials* **27**, 3413-3431. (doi:10.1016/j.biomaterials.2006.01.039)

5. Park KM, Lee SY, Joung YK,Na JS, LeeMC, Park KD. 2009. Thermosensitive chitosan–pluronic hydrogel as an injectable cell delivery carrier for cartilage regeneration. *Acta Biomater.* **5**, 1956–1965. (doi:10.1016/j.actbio.2009.01.040)
6. Norouzi M, Nazari, B, Miller DW. 2016. Injectable hydrogel-based drug delivery systems for local cancer therapy. *Drug Discovery Today* **21**, 1835–1849 (doi.org/10.1016/j.drudis.2016.07.006).
7. Haraguchi K, Takehisa T. 2002. Nanocomposite hydrogels: a unique organic–inorganic network structure with extraordinary mechanical, optical, and swelling/de-swelling properties. *Adv. Mater.* **14**, 1120–1124. (doi:10.1002/1521-4095(20020816)14:16<1120::AIDADMA1120>3.0.CO;2-9)
8. Hu Z, Chen G. 2014. Novel nanocomposite hydrogels consisting of layered double hydroxide with ultrahigh tensibility and hierarchical porous structure at low inorganic content. *Adv. Mater.* **26**, 5950–5956. (doi:10.1002/adma.201400179)
9. Lopez-Lopez MT, Duran JDG, Iskakova LY, Zubarev AY. 2016. Mechanics of magnetopolymer composites: A Review. *J. Nanofluids* **5**, 479–495. (doi: https://doi.org/10.1166/jon.2016.1233)
10. Datta P. 2018. Magnetic gels. In *Polymeric gels characterization, properties and biomedical applications*, ch. 17 (eds PK Kunal, I Banerjee), pp. 441–465. Amsterdam, The Netherlands: Elsevier.
11. Gila-Vilchez C, Mañas-Torres MC, Contreras-Montoya R, Alaminos M, Duran JDG, Álvarez de Cienfuegos L, Lopez-Lopez MT. 2019. Anisotropic magnetic hydrogels: design, structure and mechanical properties. *Phil. Trans. R. Soc. A* **377**: 20180217. (http://dx.doi.org/10.1098/rsta.2018.0217)
12. Bonhome-Espinosa AB, Campos F, Rodriguez IA, Carriel V, Marins JA, Zubarev A, Duran JDG, Lopez-Lopez MT. 2017. Effect of particle concentration on the microstructural and macromechanical properties of biocompatible magnetic hydrogels. *Soft Matter* **13**, 2928–2941. (doi:10.1039/c7sm00388a)
13. Abrougui MM, Lopez-Lopez MT, Duran JDG. 2019. Mechanical properties of magnetic gels containing rod-like composite particles. *Phil. Trans. R. Soc. A* **377**: 20180218. (http://dx.doi.org/10.1098/rsta.2018.0218)
14. Rao KM, Kumar A, Haider A, Han SS. 2016. Polysaccharides based antibacterial polyelectrolyte hydrogels with silver nanoparticles. *Mater. Lett.* **184**, 189–192. (doi.org/10.1016/j.matlet.2016.08.043)
15. Iqbal B, Muhammad N, Jamal A, Ahmad P, Khan ZUH, Rahim A, Rehman IU. 2017. An application of ionic liquid for preparation of homogeneous collagen and alginate hydrogels for skin dressing. *J. Mol. Liq.* **243**, 720–725. (doi.org/10.1016/j.molliq.2017.08.101)
16. Gila-Vilchez C, Bonhome-Espinosa AB, Kuzhir P, Zubarev A, Duran JDG, Lopez-Lopez MT. 2018. Rheology of magnetic alginate hydrogels. *J. Rheol.* **62**, 1083–1096. (doi:10.1122/1.5028137)
17. Lopez-LopezMT, Scionti G, Oliveira AC, Duran JDG, Campos A, AlaminosM, Rodriguez IA. 2015. Generation and characterization of novel magnetic field-responsive biomaterials. *PLoS ONE* **10**, e0133878. (doi:10.1371/journal.pone.0133878)
18. Seow WY, Hauser CAE. 2014. Short to ultrashort peptide hydrogels for biomedical uses. *Mater. Today* **17**, 381–388. (doi:10.1016/j.mattod.2014.04.028)
19. Contreras-Montoya R, Bonhome-Espinosa AB, Orte A, Miguel D, Delgado-Lopez JM, Duran JDG, Cuerva JM, Lopez-Lopez MT, Alvarez de Cienfuegos L. 2018. Iron nanoparticles based supramolecular hydrogels to originate anisotropic hybrid materials with enhanced mechanical strength. *Mater. Chem. Front.* **2**, 686–699. (doi:10.1039/C7QM00573C)
20. Kuo CK, Ma PX. 2001. Ionically crosslinked alginate hydrogels as scaffolds for tissue engineering: part 1. Structure, gelation rate and mechanical properties. *Biomaterials* **22**, 511–21. (https://doi.org/10.1016/S0142-9612(00)00201-5)
21. Gila-Vilchez, Duran JDG, Gonzalez-Caballero F, Zubarev A, Lopez-Lopez MT. 2019. Magnetorheology of alginate ferrogels. *Smart Mater. Struct.* **28**, 035018. (https://doi.org/10.1088/1361-665X/aafeac)
22. Abrougui MM, Bonhome-Espinosa AB, Bahri D, Lopez-Lopez MT, Duran JDG, Srasra E. 2018. Rheological properties of clay suspensions treated by hydrocyclone process. *J. Nanofluids* **7**, 258-268. (doi.org/10.1166/jon.2018.1460)

23. Abrougui MM, Bahri D, Srasra E. 2019. Structural characterizations and viscosity behavior of purified clay obtained by hydrocyclone process. *Chemistry Africa*, online 02 July 2019. (https://doi.org/10.1007/s42250-019-00076-9)
24. Liu Y, Liu P, Su Z, Li F, Wen F. 2008. Attapulgite–Fe3O4 magnetic nanoparticles via co-precipitation technique. *App Surf Sci* **255**, 2020-2025. (doi: 10.1016/j.apsusc.2008.06.193)
25. Galindo-Gonzalez C, Vicente J, Ramos-Tejada MM, Lopez-Lopez MT, Gonzalez-Caballero F, Duran JDG. 2005. Preparation and sedimentation behavior in magnetic fields of magnetite-covered clay particles. *Langmuir* **21**, 4410–4419. (doi:10.1021/la047393q)
26. Viota JL, Arroyo FJ, Delgado AV, Horno J. 2010. Electrokinetic characterization of magnetite nanoparticles functionalized with amino acids. *J. Colloid Interface Sci.* **344**, 144–149. (doi:10.1016/j.jcis.2009.11.061)
27. Duran JDG, Ramos-Tejada MM, Arroyo FJ, Gonzalez-Caballero F. 2000. Rheological and electrokinetic properties of sodium montmorillonite suspensions. *J Colloid Interface Sci.* **229**, 107–117. (doi:10.1006/jcis.2000.6956)
28. Ramos-Tejada MM, de Vicente J, Ontiveros A, Duran JDG. 2001. Effect of humic acid adsorption on the rheological properties of sodium montmorillonite suspensions. *J. Rheol.* **45**, 1159–1172. (doi:10.1122/1.1392297)
29. Ramos-Tejada MM, Ontiveros A, Viota JL, Durán JDG. 2003. Interfacial and rheological properties of humic acid/hematite suspensions. *J Colloid Interface Sci.* **268**, 85–95. (doi:10.1016/S0021-9797(03)00665-9)
30. Xua XQ, Shen H, Xu JR, Xie MQ, Li XJ. 2006. The colloidal stability and core-shell structure of magnetite nanoparticles coated with alginate. *App Surf Sci* **253**, 2158-2164. (doi:10.1016/j.apsusc.2006.04.015)
31. Benli B, Boylu F, Can MF, Karakas F, Cinku K, Ersever G. 2011. Rheological, electrokinetic, and morphological characterization of alginate-bentonite biocomposites, *J App Polym Sci* **122**, 19-28. (https://doi.org/10.1002/app.33627)
32. Jiles DC. Introduction to magnetism and magnetic materials. Chapman & Hall, London; 1991. p. 115, p. 94. (doi: 10.1088/0022-3727/27/1/001)
33. Kemp SJ, Ferguson RM, Khandhar AP, Krishnan KM. 2016. Kemp SJ, Ferguson RM, Khandhar AP, Krishnan KM. 2016. *Rsc Advanced* **6**, 77452-77464. (doi: 10.1039/c6ra12072e)
34. Rosenweig RE. Ferrohydrodynamics. Cambridge University Press, New York; 1985, p. 58. (https://doi.org/10.1002/zamm.19870670626)
35. Ginder JM, Davis LC, Elie LD. 1996. Rheology of magnetorheological fluids: models and measurements. *Int J Mod Phys* B **10**, 3293-3303. (https://doi.org/10.1142/S0217979296001744)
36. Bossis G, Volkova O, Lacis S, Menier. In: Odenbach S, editor. Magnetorheology: Fluids, structures and rheology. Springer, Bremen; 2002. Chapter 11, pp. 202–230. (doi: 10.1007/3-540-45646-5)
37. Zubarev A, Bonhome-Espinosa AB, Alaminos, Duran JDG, Lopez-Lopez MT. 2018. Rheological properties of magnetic biogels. *Arch Appl Mech* Published online: 24 August 2018. (https://doi.org/10.1007/s00419-018-1450-2)

Table 1. Description of the different samples (particles, suspensions, and ferrogels) employed.

Sample	Composition
Bent	Bentonite particles (purified by hydrocyclone process)
Fe3O4	Magnetite nanoparticles
BMag	Bare (non-functionalized) magnetite-covered bentonite particles
BMagF1	Particles functionalized by dispersion of 1 g of "BMag" particles in 50 mL of a 0.5% w/v solution of sodium alginate
BMagF2	Similar to "BMagF1" particles, but obtained by dispersion in a 2% w/v solution of sodium alginate
BMag, or BMagF1, or BMagF2 suspensions	Suspensions of the different kinds of particles in aqueous media. Particle concentration 1% w/v (zeta potential measurements) or 10% w/v (rheology)
BMagF1+X%Alg	Ferrogel containing 10% w/v of functionalized particles (BMagF1) and X% w/v of sodium alginate in the pregel solution (X = 0.25, 0.5, 1, 2)
BMagF2+X%Alg	Entirely similar to ferrogel "BMagF1+X%Alg", but containing BMagF2 particles

Table 2. Intensity of the magnetorheological effect quantified by means of eqs. [3] and [4] for the suspension, and eq. [3] for the ferrogels. The plastic viscosities (η) of the suspensions are given in mPa·s. The G′ (Pa) values correspond to a strain amplitude of 0.1 (10%).

Sample	Magnetic field intensity						
	H = 0 kA/m	H = 156 kA/m			H = 282 kA/m		
	η(0)	η(H)	Δη	MRE-η(%)	η(H)	Δη	MRE-η(%)
Suspension BMag particles (eq. 4)	90	94	4	4	168	78	87
	G′	G′	ΔG′	MRE(%)	G′	ΔG′	MRE(%)
Suspension BMag particles (eq. 3)	11	8380	8369	76100	21700	21689	197200
Ferrogel BMagF2+0.25%Alg	915	1687	772	84	2442	1527	167
Ferrogel BMagF2+0.5% Alg	920	2585	1665	181	5708	4788	520
Ferrogel BMagF2+1% Alg	8187	8501	323	4	9929	1751	21
Ferrogel BMagF2+2%Alg	39310	41020	1710	4	43920	4610	12

Table 3. Comparison among the magnetorheological effects, calculated by equations [3] and [5], achieved by ferrogels that contain particles with different shapes and compositions.

Ferrogel (reference)	Composition (Particle shell-core /Polymer in hydrogel)	M_S (kA/m)	H (kA/m)	Φ (% v/v)	MRE (%)	$\overline{MRE}$(%)
BMagF2+0.5% Alg	Platelets Fe_3O_4-bentonite /Alginate (0.5% w/v)	110 [a]	282 [a]	4.05 [a]	520	520
Ferrogel BMagF2+1% Alg	Platelets Fe_3O_4-bentonite /Alginate (1% w/v) [b]	110 [a]	282 [a]	4.05 [a]	21	21

Ferrogel-1 Ref. [13]	Fibre-like Fe_3O_4-sepiolite /Alginate (1% w/v) [b]	169.9	282	0.93	64	180
Ferrogel Ref. [16] [c]	Spherical silica-Fe /Alginate (1% w/v) [b]	1587	282	4.6	700	43
Ferrogel Refs. [37] [c]	Spherical polymer-Fe_3O_4 / Fibrin-agarose	161	48.6	3.5	8	37

[a] $M_{S,0}$, $H_{max,0}$, Φ_0 in equation [5]; [b] alginate concentration in pregel solution 1% w/v; [c] see also ref. [13]

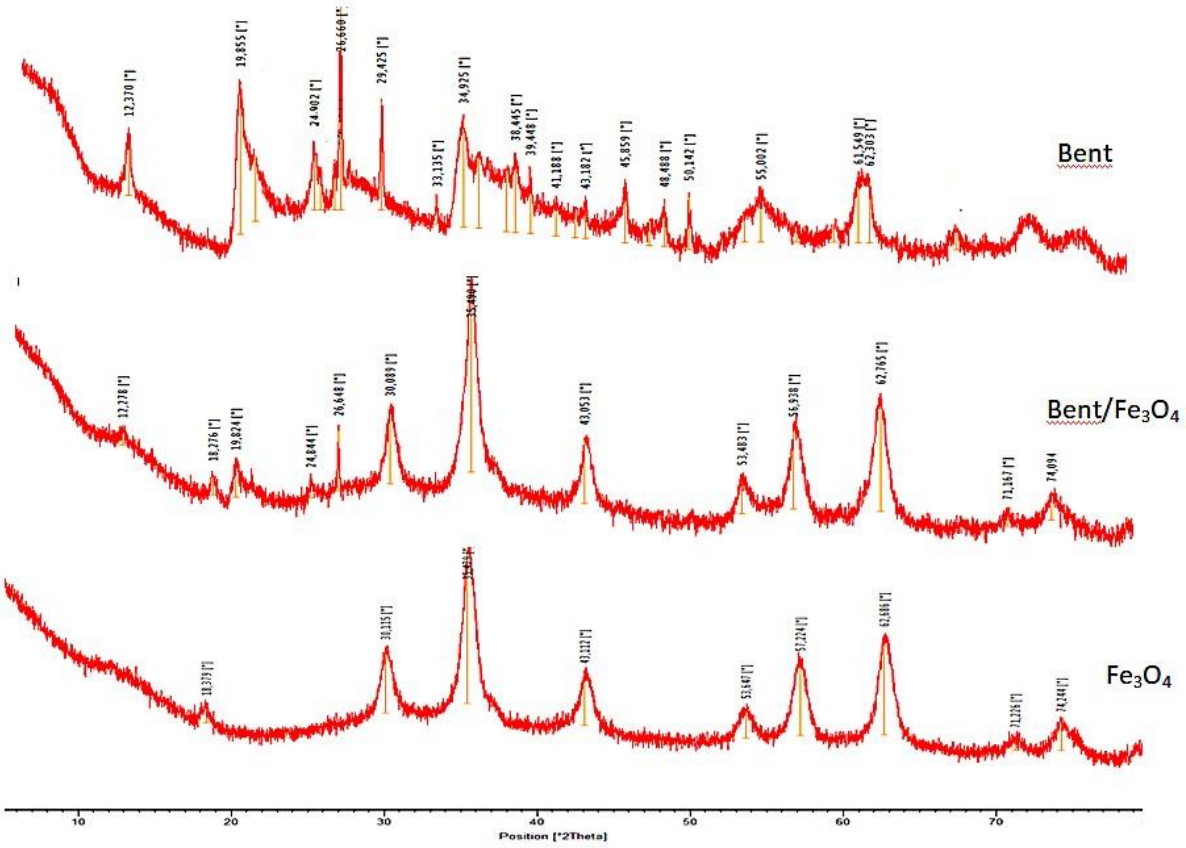

Figure 1. XRD patterns of bentonite (Bent), magnetite-covered bentonite (Bent/Fe_3O_4), and magnetite particles.

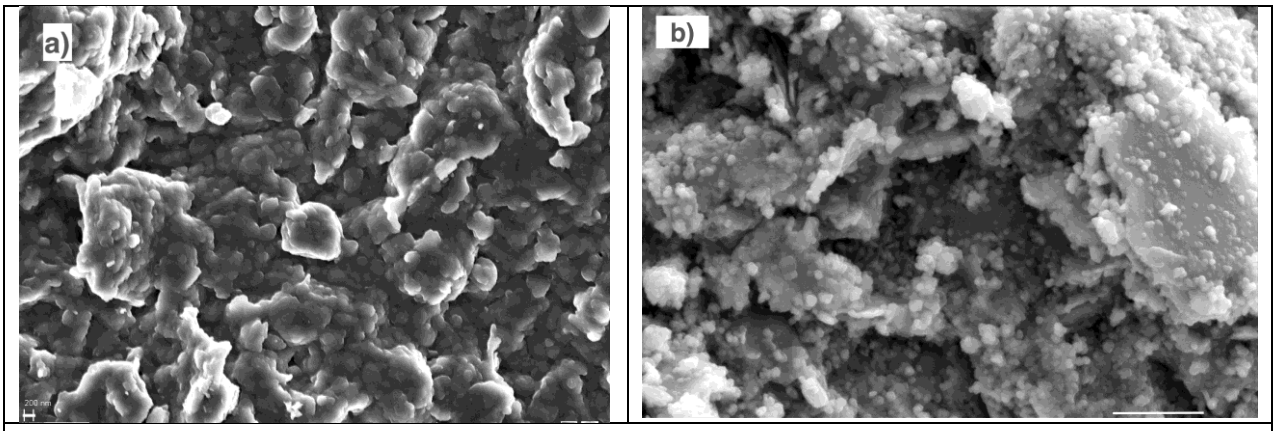

Figure 2. Pictures obtained by SEM of Bent (a), and BMag (b) particles. Bar lengths: a) 200 nm (short line in the lower left corner), b) 1 μm (line in the lower right corner).

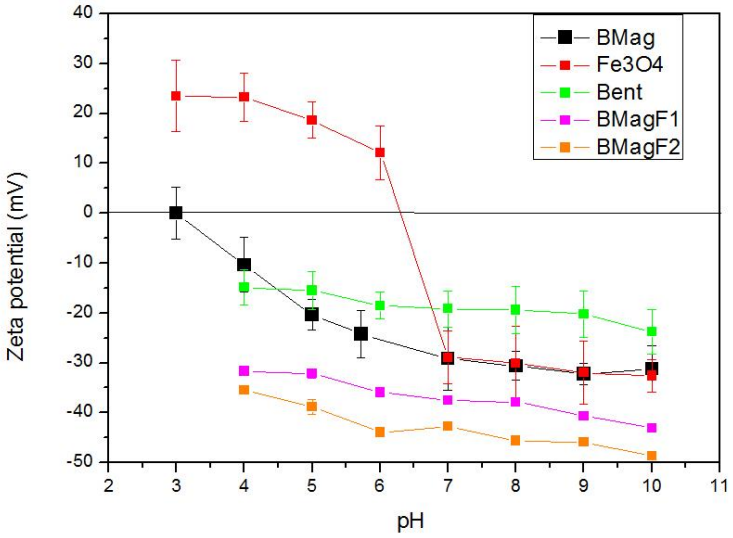

Figure 3. Zeta potential of the indicated particles in aqueous suspensions (see Table 1) as a function of the pH of the aqueous medium. Particle concentration 1% w/v. Ionic strength of the solutions 1 mM NaCl.

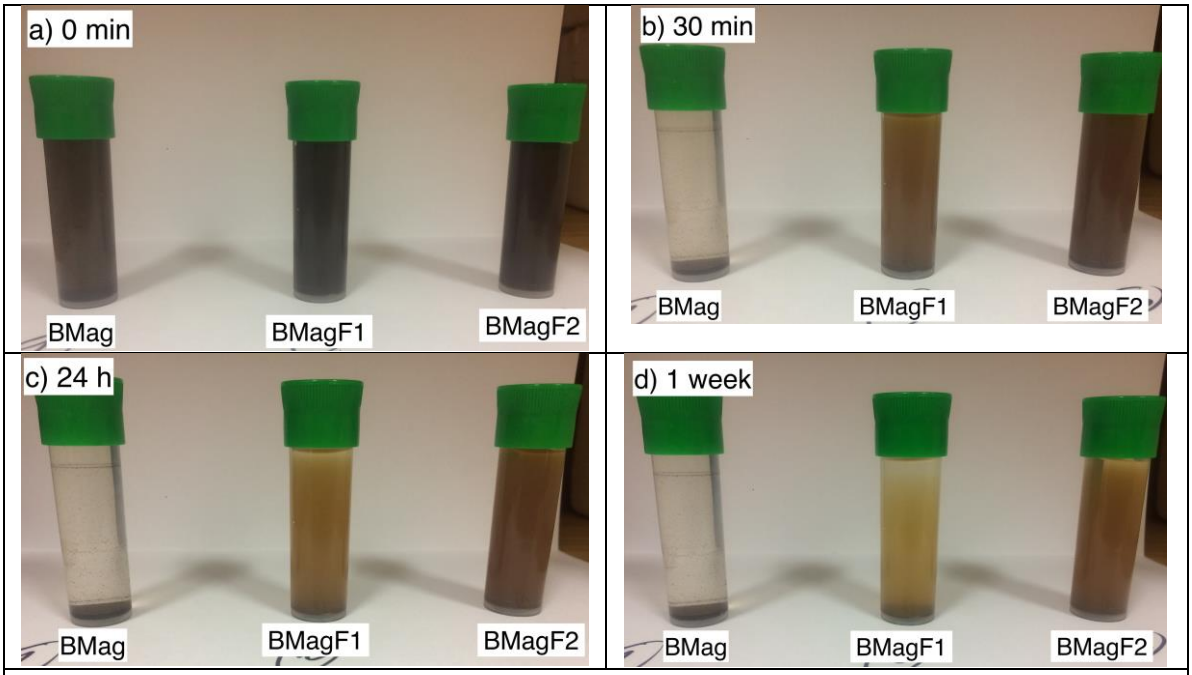

Figure 4. Sedimentation of the suspensions of bare (BMag) and functionalized (BMagF1, BMagF2) composite particles. The indicated times correspond to those elapsed from preparation and strong redispersion of the samples. Particle concentration 1% w/v. Ionic strength of the solutions 1 mM NaCl.

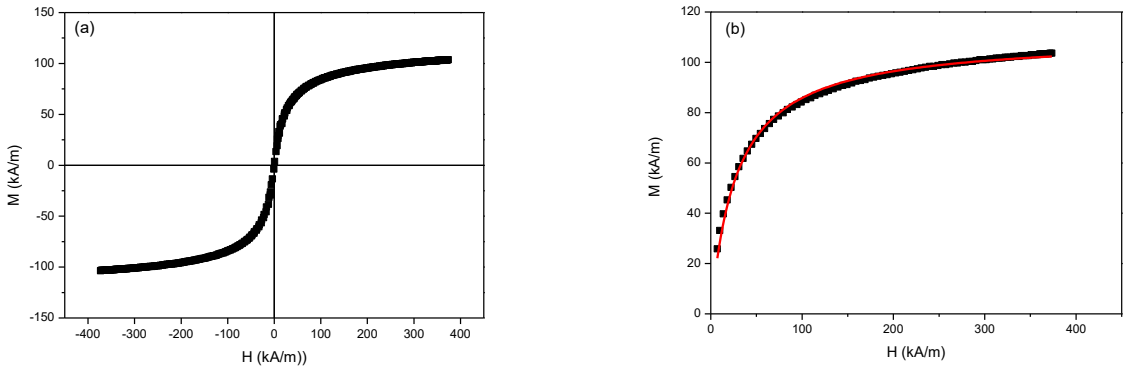

Figure 5. a) Magnetization loop of magnetite-covered bentonite particles (sample BMag). b) First magnetization curve of BMag powder; the red line is the fitting to Frölich-Kennely equation, eq. [1].

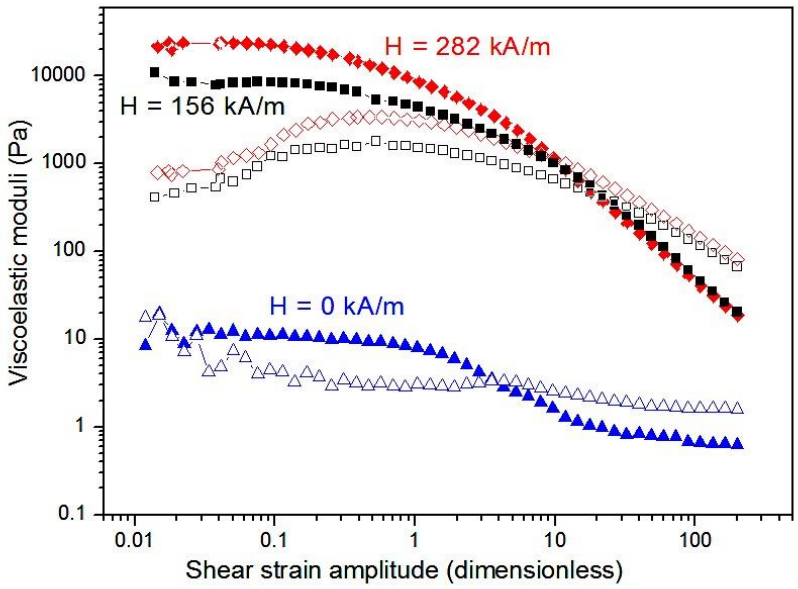

Figure 6. Viscoelastic moduli as a function of the strain amplitude of the aqueous suspension of BMag particles in the absence/presence of the indicated magnetic fields (H). Particle concentration 10% w/v. Solid symbols: elastic modulus, G'; open symbols: viscous modulus, G".

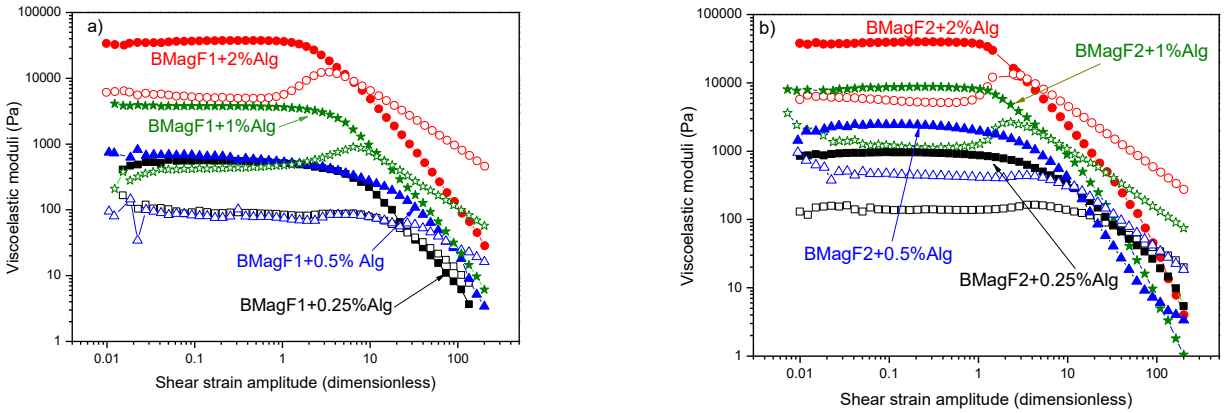

Figure 7. Viscoelastic moduli, in the absence of magnetic field, as a function of the strain amplitude for the different hydrogels prepared. a) Hydrogels BMagF1+X%Alg (see Table 1). b) Hydrogels BMagF2+X%Alg (Table 1). Solid symbols: G'; open symbols: G".

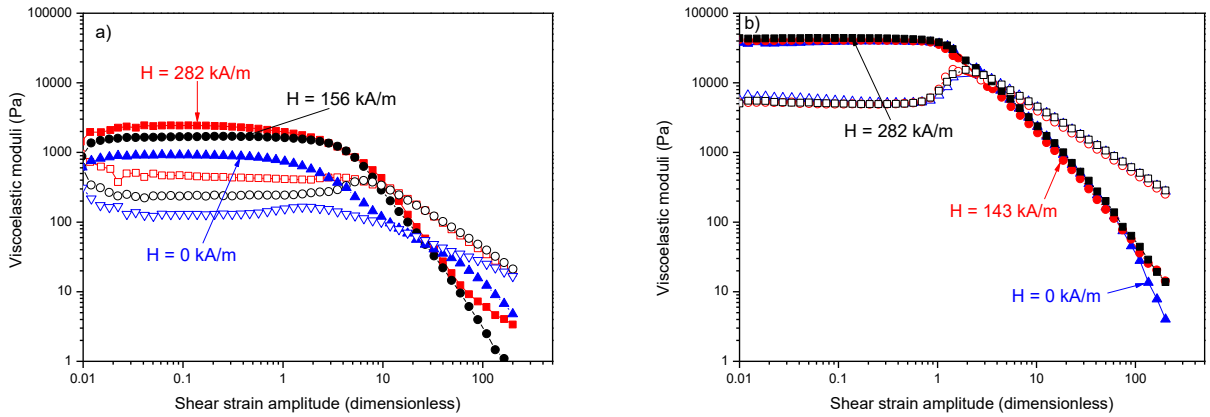

Figure 8. Viscoelastic moduli as a function of the strain amplitude of hydrogels BMagF2+X%Alg (see Table 1). a) Sample BMagF2+0.25%Alg. b) Sample BMagF2+2%Alg. The values of the magnetic field applied are indicated. Solid symbols: elastic modulus, G'; open symbols: viscous modulus, G".